MEDICAL SCIENCE MONITOR

ANIMAL STUDY

e-ISSN 1643-3750
© Med Sci Monit, 2018; 24: 1624-1632
DOI: 10.12659/MSM.905654

Received: 2017.06.06
Accepted: 2017.09.02
Published: 2018.03.19

Characteristics of Pulmonary Vascular Remodeling in a Novel Model of Shunt-Associated Pulmonary Arterial Hypertension

Authors' Contribution:
Study Design A
Data Collection B
Statistical Analysis C
Data Interpretation D
Manuscript Preparation E
Literature Search F
Funds Collection G

BE Mingjie Zhang
C Zhiyu Feng
D Rui Huang
F Chongrui Sun
ABC Zhuoming Xu

Department of Cardiothoracic Surgery, Shanghai Children's Medical Center, Shanghai Jiaotong Universtiy School of Medicine, Shanghai, P.R. China

Corresponding Author: Zhuoming Xu, e-mail: zmxyfb@163.com
Source of support: Sponsored by Natural Science Foundation of Shanghai (15ZR1427100)

Background: Establishing a shunt-induced pulmonary arterial hypertension (PAH) model in mice would be of great scientific value, but no such models have been reported to date. Here, we established a shunt-associated PAH in mice to investigate the characteristics of pulmonary vascular remodeling, which provides a new platform for the in-depth study of PAH associated with congenital heart disease (CHD).

Material/Methods: Eighty mice were randomly divided into the heavy shunt group (n=32), the small shunt group (n=32), the sham operation group (n=8), and the control group (n=8). The septum of the abdominal aorta and inferior vena cava was cut directly to create a heavy abdominal aortocaval shunt. Pulmonary artery pressure, right ventricular hypertrophy index, and lung tissue morphology were evaluated in the 4th, 6th, 8th, and 12th weeks in the shunt groups.

Results: Shunt-associated PAH by abdominal aortocaval shunt in mice was successfully established. The shunt patency rate was significantly higher in the heavy shunt group. Significant differences were observed between the heavy shunt group and other groups in terms of pulmonary artery pressure and the right ventricular hypertrophy index. Tissue sections revealed a thickened pulmonary intimal layer and muscular layer and stenosis of the lumen in the shunt groups. Immunofluorescent assay results showed significant proliferations of PAH smooth muscle cells and endothelial cells, consistent with the clinical pulmonary vascular remodeling seen in human patients with severe PAH.

Conclusions: Shunt-associated PAH established by directly cutting the septum between the abdominal aorta and inferior vena cava is a stable and reliable model for research on PAH associated with CHD.

MeSH Keywords: Arteriovenous Shunt, Surgical • Heart Defects, Congenital • Hypertension, Pulmonary • Models, Animal

Full-text PDF: https://www.medscimonit.com/abstract/index/idArt/905654

3044 2 5 26

Indexed in: [Current Contents/Clinical Medicine] [SCI Expanded] [ISI Alerting System] [ISI Journals Master List] [Index Medicus/MEDLINE] [EMBASE/Excerpta Medica] [Chemical Abstracts/CAS]

Background

Pulmonary artery hypertension (PAH) is a common complication of the left-to-right shunt type found in congenital heart disease (CHD). About 5–10% of CHD patients have varying degrees of PAH [1,2]. Reportedly, of every 5500 patients with CHD, 400–500 have PAH that requires treatment [3]. In CHD-related pulmonary hypertension, shunt-associated PAH is the most common subtype.

In the past, surgeries were often performed on pigs and other large animals to simulate the pathophysiology of shunt-induced PAH [4]. Researchers established a systemic-to-pulmonary shunt through artificial vascular to increase the lateral lobe artery pressure; however, it was difficult to control the shunt volume, and the artificial blood vessels tended to distort, resulting in luminal stenosis or occlusion [4]. Some scholars have successfully established a PAH model by using abdominal aortocaval shunts in rats, and they provided a new way to study shunt-induced PAH [5]. This important innovation provides an available model with a clearly mapped genetic background to study cellular interactions, signal pathways, and gene expressions involved in PAH [6–9]. Furthermore, transgenic and knockout mice have been developed in recent years, providing greater opportunities for studying the molecular mechanisms in PAH. Establishing a shunt-induced PAH model in mice would be of great scientific value, but no such models have been reported to date [10–15].

Our study aimed to establish a PAH model in mice by establishing an abdominal aortocaval shunt that is consistent with the physiological and pathological characteristics of human cases of CHD-associated PAH, which would provide a reliable platform for studying CHD-associated PAH in humans.

Material and Methods

Experimental animals

All the animal care and experiments were performed in accordance with the Guide for the Care and Use of Animals of the Laboratory Animal Center of Shanghai Jiaotong University, School of Medicine. The local committee on animal experimentation approved this study. Eighty healthy male C57BL/6J mice (Shanghai Silaike Experiment Animal Co., Ltd.) weighing 20–30 g were used. The animal rating was a clean grade specific pathogen-free, and the experimental animal licenses were SCXK (Shanghai) 2007-0005 and SYXK (Shanghai) 2003-0026. The animals were housed 5 per cage. Food and water were freely available at all times, and a temperature-controlled room (21°C; relative humidity, 50–80%) was maintained on a normal light cycle. The animals were randomly divided into a small shunt group (n=32, the 4th, 6th, 8th, and 12th week groups), heavy shunt group (n=32, the 4th, 6th, 8th, and 12th week groups), sham operation group (n=8), and control group (n=8).

Establishing the animal model

The C57BL/6J mice (4 weeks old) were weighed and intraperitoneally anesthetized with 80 mg/kg of 1% sodium pentobarbital. The abdomen was incised to expose the abdominal aorta and inferior vena cava (Figure 1A). Both sides of the free branch vessels were ligated under a microscope, and 6-0 polyester filaments were used to block the abdominal aorta and the inferior vena cava together between the left renal artery and the iliac artery. Micro-scissors with a curved tip were used to make a transverse incision in the anterior wall of the abdominal aorta to expose the contralateral wall, which is adjacent to the wall of the inferior vena cava (Figure 1B).

A longitudinal incision was made in the interval of the abdominal aorta and the inferior vena cava to establish an aortocaval shunt by use of micro-scissors. The incision length was half of the diameter of the abdominal aorta. To determine whether the shunt was made, normal saline was injected from the abdominal aorta, and the inferior vena cava would be filled with normal saline (Figure 1C). After the shunt was made, 11-0 polypropylene monofilament was used to suture the incision in the abdominal aorta wall. Then, the blocking filament was loosened. The inferior vena cava pulsed and was swollen with arterial blood, confirming the presence of a shunt (Figure 1D).

To establish the small shunt group, a 30-G needle was inserted into the incision, punctured through the abdominal aorta wall, and entered the adjacent inferior vena cava at a different direction to expand the fistula and create multiple fistulas.

The sham operation group did not have an arteriovenous shunt, so the anterior wall of the abdominal aorta was sutured immediately after the incision.

No treatment was performed in the control group, and these mice were fed and raised under normal conditions.

Evaluating the pulmonary artery pressure

The mice were anesthetized and intubated by directly cutting the trachea. The small animal ventilator parameters were set to a frequency of 120 beats/min and a tidal volume of 0.15 ml (6–8 ml/kg) with a 21% inhaled oxygen concentration. The chest skin was quickly cut and opened along the center of the sternum. The pericardium was cut to expose the right ventricle. A polyethylene catheter infused with a heparin solution was connected to one end of a pressure transducer to record

Indexed in: [Current Contents/Clinical Medicine] [SCI Expanded] [ISI Alerting System] [ISI Journals Master List] [Index Medicus/MEDLINE] [EMBASE/Excerpta Medica] [Chemical Abstracts/CAS]

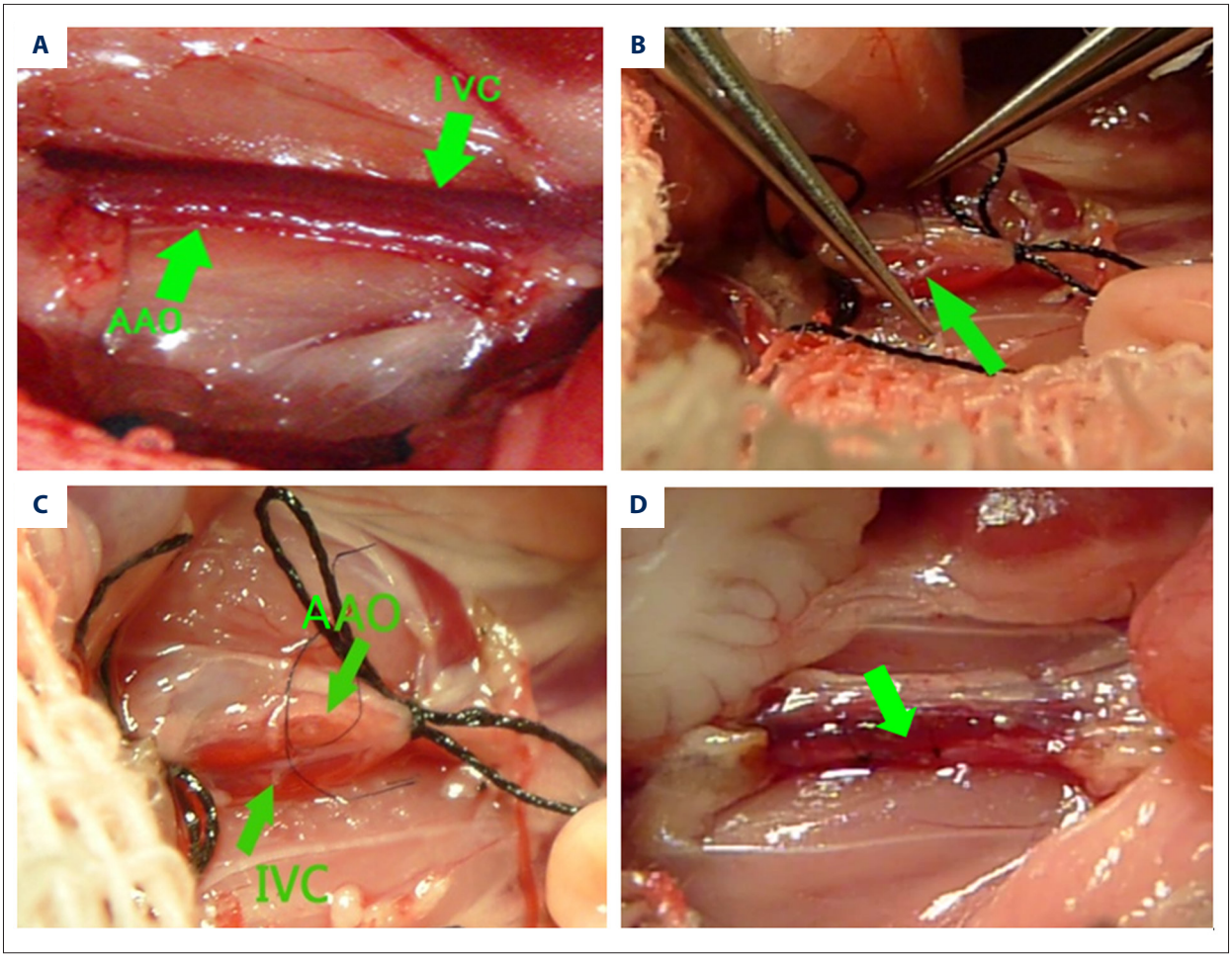

Figure 1. Surgical procedure of creation of the shunt. (**A**) The abdominal aorta (AAo) and inferior vena cava (IVC) were tightly linked together; (**B**) Blood in the abdominal aorta and the inferior vena cava were blocked and a transverse incision were made in the abdominal aorta's anterior wall to expose the contralateral wall, and then the wall were cut by micro-scissors; (**C**) Normal saline was injected from the abdominal aorta and the inferior vena cava was filled with normal saline; (**D**) After the shunt was made, the inferior vena cava pulsed with arterial blood.

the pressure curve, while the other end was connected to a 27-G needle, which punctured the right ventricle along the right ventricular outflow. Data were recorded when the pressure waveform was stable. The right ventricular systolic pressure was used to represent the systolic pulmonary artery pressure (sPAP). The sPAP was measured in the shunt groups at the end of the 4th, 6th, 8th, and 12th weeks postoperatively, which was measured in the sham operation and control groups at the end of the 12th week.

Evaluating the right ventricular hypertrophy index

Followed by the sPAP measurement, the bilateral superior vena cava, inferior vena cava, and aorta were ligated, and the heart and lungs were rapidly removed. When the needle punctured the right ventricular outflow to infuse the lungs with saline, the color of the blood flowing from the aorta continuously faded until the lungs eventually turned completely white. The atrium and major vessel roots were cut along the atrioventricular groove. The free right ventricular wall along the groove of the posterior ventricle was separated. A precision electronic scale was used to weigh the right ventricular free wall (RV) and the left ventricle free wall plus the septum (LV + S). The weight ratio of the RV to the LV + S was calculated to obtain the right ventricular hypertrophy index (RVHI). The RVHI was measured in the shunt groups at the end of 4th, 6th, 8th, and 12th weeks postoperatively, which was measured in the sham operation and control groups at the end of 12th week.

Pathological changes

At least 5 small muscular arteries with complete internal and external elastic lamina were randomly selected from the lung tissue sections in the surviving mice in each group, stained

Indexed in: [Current Contents/Clinical Medicine] [SCI Expanded] [ISI Alerting System] [ISI Journals Master List] [Index Medicus/MEDLINE] [EMBASE/Excerpta Medica] [Chemical Abstracts/CAS]

with van Gieson's stain, and the inner and outer elastic lamina contours were outlined with a cursor within an Axioplan 2 microscope imaging analysis system (Carl Zeiss). The medial thickness (MT), vascular external diameter (ED), and vascular internal diameter (ID) of the internal and external elastic lamina were measured. The average medial thickness percentage (MT%) of the pulmonary arterioles was further calculated as MT%=(2×MT÷ED)×100.

Immunofluorescence assays on the lung tissue sections

The mice lung tissue sections were placed in the retrieval box filled with ethylene diamine tetraacetate antigen retrieval buffer (pH, 9.0), and antigen retrieval was performed in the microwave. The samples were boiled under medium heat followed by a 10-min interval. During this process, excessive evaporation of the buffer was prevented to avoid drying the sample. After cooling naturally, the samples were loaded onto slides, placed in a phosphate-buffered saline (PBS) (pH, 7.4) solution, and washed 3 times for 5 min each on a shaker to rinse the stain. After drying, the tissue surroundings were outlined with a marker, and 5% bovine serum albumin diluted rabbit anti-mouse CD31 antibody and rabbit anti-mouse α-SMA antibody were added to cover the tissues. The slices were placed flat in a humidified box and were incubated overnight at 4°C. Then, the slides received PBS (pH, 7.4) and were placed on a shaker 3 times for 5 min each to wash. After slightly drying, the secondary antibody, a goat anti-rabbit fluorescein isothiocyanate fluorescence, was added to cover the tissue samples. The samples were incubated in the dark at room temperature for 50 min. Next, the slides received PBS (pH, 7.4) and were placed on a shaker for 3 cycles of 5 min each to wash out. After slightly drying, 4',6-diamidino-2-phenylindole dye was added to the slices, and the samples were incubated in the dark at room temperature for 10 min. Each slide received PBS (pH, 7.4) and was placed on the shaker for 3 cycles of 5 min each to wash out the stain. After slightly drying, the antifade solution was added to the slices, and the samples were mounted and sealed. The samples were analyzed under a Nikon inverted fluorescence microscope to acquire images and perform image processing.

Statistical analysis

SPSS version 16.0 statistical software (SPSS, Inc.) was used to perform the statistical analyses. All data are presented as a mean ± standard deviation (x±s). Mixed linear regression for repeated measures was used to determine the nature of any time trend in the variables. Data for multiple samples were compared using multiple analyses of variance between the groups. The chi-square test was used for quantified data. A P-value <0.05 was considered significant.

Results

Survival and growth

A mouse in the heavy shunt group died from excessive bleeding on the operating table, and a mouse in the small shunt group had lower limb paralysis and died on the second day after surgery. Two mice in the heavy shunt surgery group died during the 10th and 11th weeks. All the mice in the sham operation and control groups survived. Mice in the shunt groups had higher mortality than those in other groups (P=0.025) (Figure 2A). Mice in the heavy shunt group had significantly reduced weight at the end of the 8th and 12th weeks compared with the mice in the small shunt group (P=0.002 and 0.017, respectively). Mice in the sham operation and control groups had no significant difference in weight during each week. Mice in both shunt groups had significantly reduced weights at the end of the 6th, 8th, and 12th weeks compared with the control group (P=0.015) (Figure 2B).

Comparison of the shunt patency

The anterior wall of the abdominal aorta was cut longitudinally and a bougie was used to test whether the shunt was still open. None had an aortocaval shunt closed in the heavy shunt group but 4 mice had aortocaval shunt closed in the small shunt in the 4th week group. Only 1 mouse had an aortocaval shunt closed in the 6th, 8th, and 12th week group in the heavy shunt group, but 5 mice had an aortocaval shunt closed in the 6th week and 6 mice had aortocaval shunt closed in the 8th and 12th week group. In addition, the rate of the shunt patency was 83.3% in the heavy shunt group in the 12th week, but it was only 25% in the small shunt group. The patency rate in the heavy shunt group was significantly higher than that in the small shunt group (Table 1).

Changes in mouse sPAP and RVHI

With the duration of the shunt was prolonged, the sPAP and RVHI of mice in both shunt groups gradually increased. Mice in the heavy shunt group had a significantly higher systolic pulmonary artery pressure (sPAP) at the end of the 12th week compared to that in the small shunt group (36.9±2.2 mmHg *vs.* 25.9±2.6 mmHg, P=0.015). Mice in the sham group had lower sPAP (11.7±1.3 mmHg) in the 12th week and sPAP (12.1±1.5 mmHg) in the control group. Mice in both shunt groups had a significantly higher sPAP at the end of the 12th weeks compared to the control and sham groups (P=0.007) (Figure 3A).

Mice in the heavy shunt group had a significantly higher right ventricular hypertrophy index (RVHI) at the end of the 12th week compared to that in the small shunt group (47.2±3.5% *vs.* 39.1±2.5%, P=0.037). Mice in the sham group had lower

Indexed in: [Current Contents/Clinical Medicine] [SCI Expanded] [ISI Alerting System] [ISI Journals Master List] [Index Medicus/MEDLINE] [EMBASE/Excerpta Medica] [Chemical Abstracts/CAS]

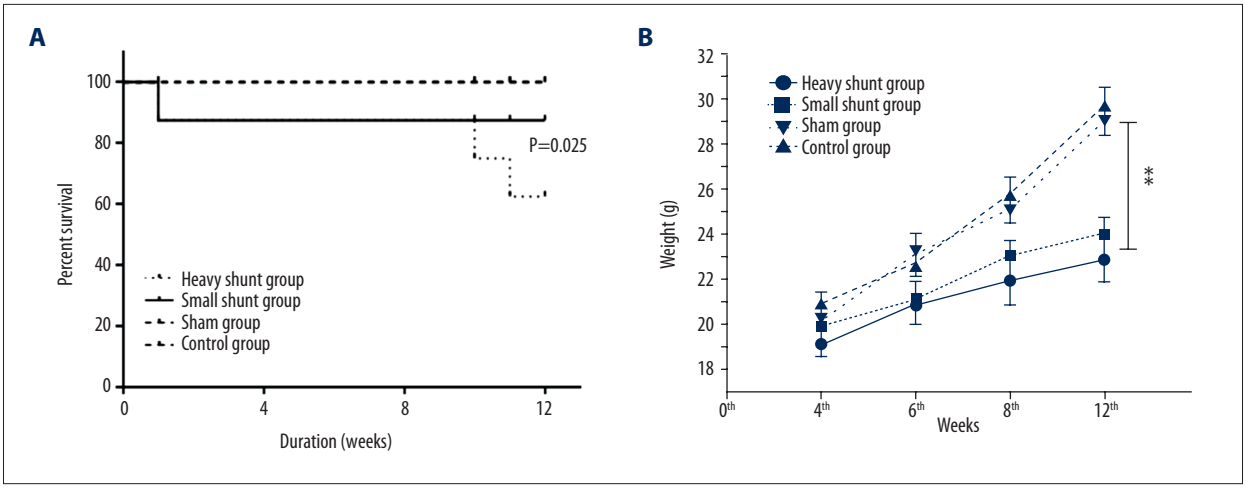

Figure 2. Survival and growth in each group. Three mice in the heavy shunt group and 1 in the small shunt group died after the shunt was established. All mice in the sham operation and control groups survived. Mice in the heavy shunt group had higher mortality than those in other groups (P=0.025) (**A**). Mice in the heavy shunt group had significantly reduced weight at the end of the 8th and 12th weeks compared to mice in the small shunt group (P=0.002 and 0.017, respectively). Mice in both shunt groups had significantly reduced weights at the end of the 6th, 8th, and 12th weeks compared to the control and sham groups (P=0.015) (**B**). (** indicate P≤0.05).

Table 1. Comparison of the patency in the shunt groups.

	Heavy shunt group (patent/closed)	Small shunt group (patent/closed)	χ^2	P
4th week	100% (8/0)	42.85% (3/4)	6.23	0.013
6th week	87.5% (7/1)	37.5% (3/5)	4.27	0.039
8th week	87.5% (7/1)	25% (2/6)	6.35	0.012
12th week	83.3% (5/1)	25% (2/6)	4.60	0.031

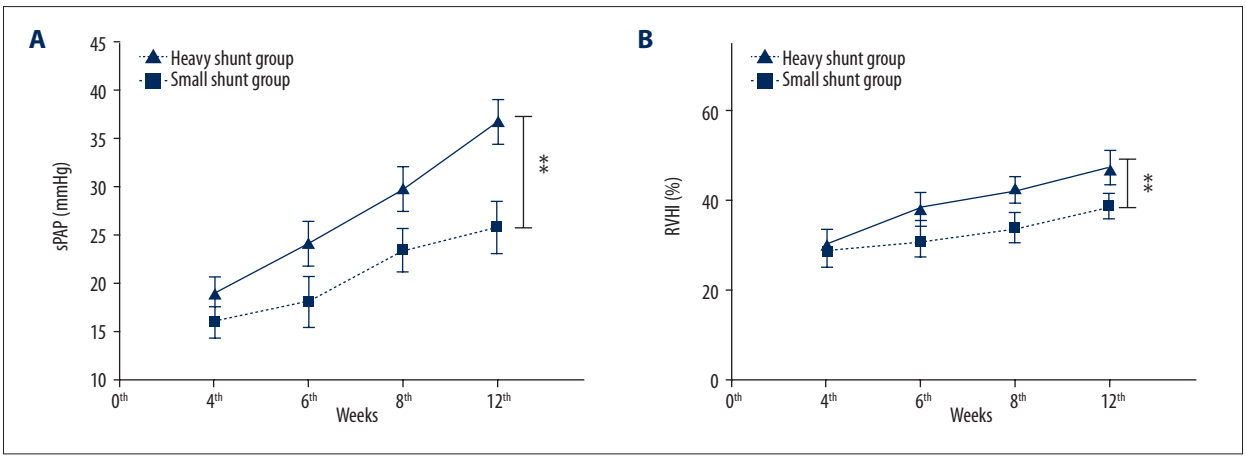

Figure 3. A comparison of the sPAP and RVHI in the shunt groups. Mice in the heavy shunt group had a significantly higher systolic pulmonary artery pressure (sPAP) at the end of the 12th week compared to that in the small shunt group (36.9±2.2 mmHg *vs.* 25.9±2.6 mmHg, P=0.015) (A). Mice in both shunt groups had a significantly higher sPAP at the end of the 12th week compared to the control and sham groups (P=0.007). Mice in the heavy shunt group had a significantly higher right ventricular hypertrophy index (RVHI) at the end of the 12th week compared to that in the small shunt group (47.2±3.5% *vs.* 39.1±2.5%, P=0.037). Mice in both shunt groups had a significantly higher RVHI at the end of the 12th week compared to the control and sham groups (P=0.02) (B). (** Indicates P≤0.05)

Indexed in: [Current Contents/Clinical Medicine] [SCI Expanded] [ISI Alerting System] [ISI Journals Master List] [Index Medicus/MEDLINE] [EMBASE/Excerpta Medica] [Chemical Abstracts/CAS]

Table 2. Comparison of the medial thickness percentage (MT%) in each group ($\bar{\chi}$±s, N=76).

	4th week	6th week	8th week	12th week
Heavy shunt	16.1±3.2	21.7±2.9	34.1±3.5	58.1±3.3
Small shunt	17.2±2.5	20.1±2.8	29.9±3.3	38.6±3.4
Sham	–	–	–	19.8±2.7
Control	–	–	–	18.5±3.1

RVHI (9.7±0.5%) in the 12th week and RVHI (8.6±0.7%) in the control group. Mice in both shunt groups had a significantly higher RVHI at the end of the 12th weeks compared to the control and sham groups (P=0.02) (Figure 3B)

Pulmonary pathological changes

In the control and sham groups, the walls of the pulmonary vessels were thin and the intima and media were difficult to distinguish. With increased duration of the shunt, the medial thickness percentage (MT%) of the heavy shunt group gradually increased, from 16.1±3.2% at the end of the 4th week to 58.1±3.3% at the end of the 12th week. The MT% was significantly higher in the heavy shunt than in the small shunt group (P<0.05) (Table 2). Compared to the mild proliferation of vascular smooth muscle cells (VSMCs) in the small shunt group, the proliferation in the heavy shunt group was more obvious. Endothelial cell proliferation only appeared in the heavy shunt group in the 12th week (Figures 4, 5).

Discussion

Studies have shown that the presence of a left-to-right shunt in CHD increases right cardiac output, causing high blood flow and a high shearing force within the pulmonary vessels, which ultimately results in vascular remodeling through a variety of mechanisms [16,17]. In this study, mice showed weight loss in the 6th week postoperatively. Increased sPAP and RVHI were observed 4 weeks after the shunt surgery, and the morphological analysis showed an increased WT%. Pulmonary artery morphology showed pulmonary vascular remodeling, which was indicated by the thickening of the artery wall in the early stage and endothelial proliferation at a more advanced stage.

The aortocaval shunt is relatively widely applied and was first described by Garcia and later modified by others [18]. Dickinson et al. [14] suggested that the success of fistula formation can be improved through repeated, multidirectional punctures in rats. In our study, we found that simply changing the direction of the puncture in the same location still caused the fistula to close in the small shunt group. We speculated that this may be a result of the one-way valve formed by the needle puncture. However, if we directly cut the interval of the inferior vena cava and the abdominal aorta, the shunt can be open longer. Similarly, Linardi et al. used an 18-gauge Neo Delta Ven 2 catheter (DeltaMedMantova, Italy), a common peripheral venous catheter, puncturing the posterior aortic wall up to the adjoining inferior vena cava, and then advancing the catheter into the inferior vena cava to create heavy shunts in rats [19]. However, murine models offer greater molecular certainty than rat models. Mouse models have been widely used and extended to genetic studies of pulmonary vascular remodeling caused by hypoxia or monocrotaline, but are rarely used in shunt-induced pulmonary arterial hypertension due to the limits of surgical techniques to create the shunt.

In a study of carotid artery-jugular vein shunt PAH model of rats, sPAP increased significantly (37.69±3.00 mmHg) compared with control group (25.41±2.08 mmHg, P<0.0001) [20]. In contrast to rat models, Chen [21] reported that mice overexpressing connective tissue growth factor generate modest PAH (average sPAP 22 mmHg *vs.* 10 mmHg in controls) but develop significant right ventricular hypertrophy (RV/LV+S 0.42), but they rarely developed right ventricular failure. Similarly, humans with Eisenmenger's syndrome develop severe PAH and right ventricular hypertrophy but do not develop signs or symptoms of right ventricular failure [22]. In our study, mice in the heavy shunt group had significantly higher sPAP (36.9±2.2 mmHg) and RVHI (47.2±3.5%), which is higher than those reported in transgenic mice [21].

Two major complications from shunting are bleeding and paralysis. Bleeding can lead to paralysis of the legs. In addition, prolonged blocking, a heavy shunt, and abdominal aortic stenosis after suturing can also lead to paralysis of the legs. Therefore, the ratio of the shunt size to the diameter of the abdominal aorta was controlled in order to adjust the volume of the shunt. In our study, the shunt size was half of the diameter of the abdominal. Keeping the blocking time within 1 h can prevent paralysis, and transversely incising the abdominal aorta rather than making a vertical incision can prevent stenosis.

Our study also showed VSMCs remodeling of the pulmonary vessels in the heavy and small shunt groups; however, ECs hyperplasia was only observed in the heavy shunt group [17].

Indexed in: [Current Contents/Clinical Medicine] [SCI Expanded] [ISI Alerting System] [ISI Journals Master List] [Index Medicus/MEDLINE] [EMBASE/Excerpta Medica] [Chemical Abstracts/CAS]

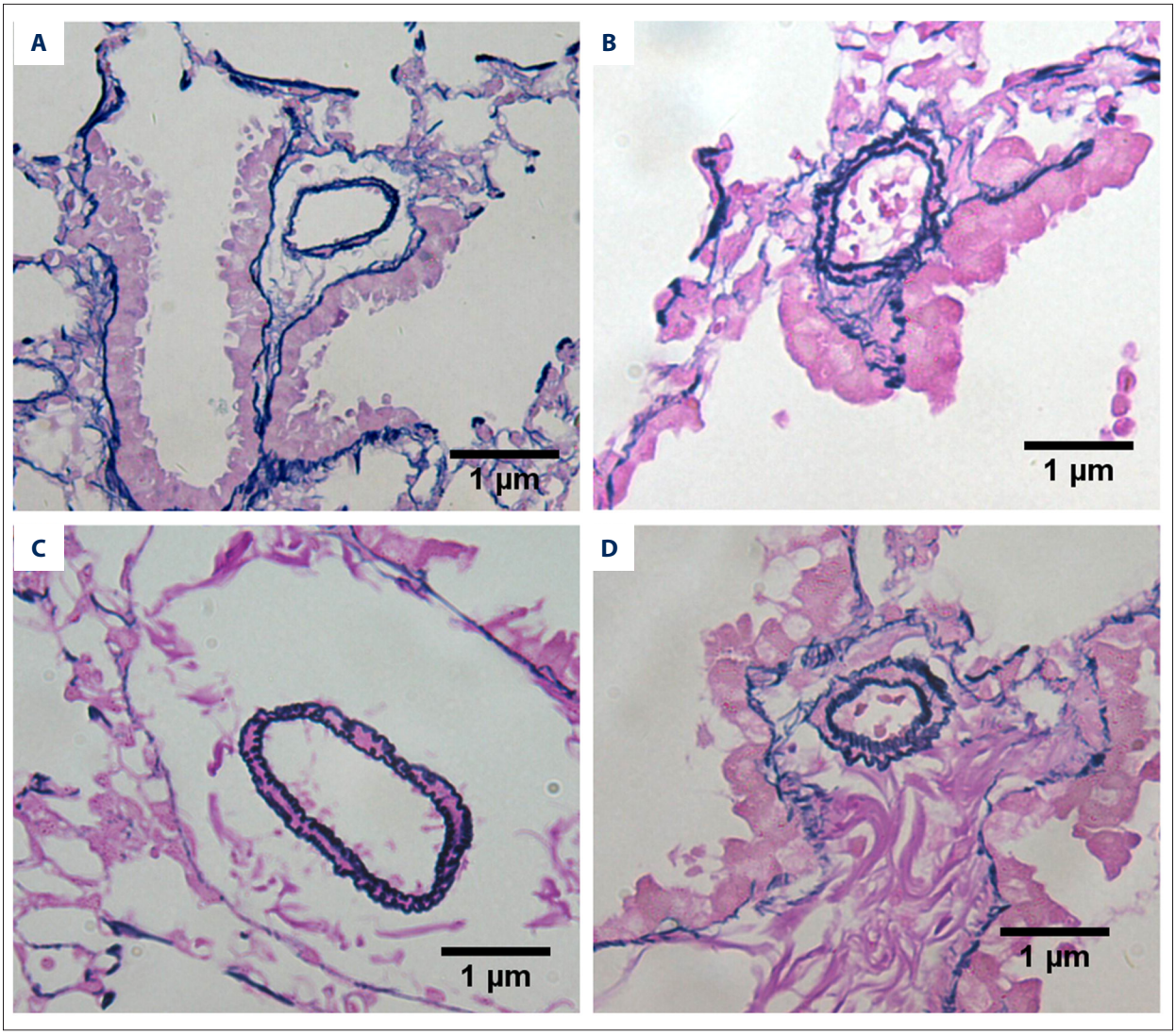

Figure 4. Pulmonary vascular remodeling in each group. (**A**) Pulmonary vascular remodeling in the 8th week (×400) showing mild proliferation of smooth muscle cells in the small shunt group; (**B**) Pulmonary vascular remodeling in the 8th week (×400) showing moderate proliferation of smooth muscle cells in the heavy shunt group; (**C**) Pulmonary vascular remodeling in the 12th week (×400) showing moderate proliferation of smooth muscle cells in the small shunt group; and (**D**) Pulmonary vascular remodeling in the 12th week (×400) showing proliferation of endothelial cells in the heavy shunt group.

Studies have shown that ECs impaired by high shear stress can release a variety of growth factors, such as vascular endothelial growth factor, which induces proliferation and hypertrophy of VSMCs [3,17]. In a clinical lung biopsy study in patients with CHD-associated PAH, intimal damage was only observed in the pulmonary vessels of patients with irreversible PAH [17]. Further investigations revealed that the anti-apoptotic protein Bcl-2 was expressed in the pulmonary vascular ECs of irreversible PAH [23]. Impaired ECs secrete vascular endothelial growth factor, which binds to ECs receptors on adjacent vessels, causing proliferation of ECs and the formation of new small vessels within the irreversible PAH pulmonary vascular wall [24]. Therefore, the dysfunction of proliferation and apoptosis of VSMCs and ECs are important pathophysiological factors for shunt-associated PAH vascular remodeling. Nevertheless, the key molecules and signaling pathway that regulate these cellular activities remain unclear [25].

Limitations

Assessing the presence of PAH by echocardiogram should be part of the protocol when studying mouse models of PAH because right ventricular catheterization is very challenging in mice. Although we obtained some hemodynamics parameters by opening the heart in our study, noninvasive tools such as echocardiography may be more helpful [26].

Indexed in: [Current Contents/Clinical Medicine] [SCI Expanded] [ISI Alerting System] [ISI Journals Master List] [Index Medicus/MEDLINE] [EMBASE/Excerpta Medica] [Chemical Abstracts/CAS]

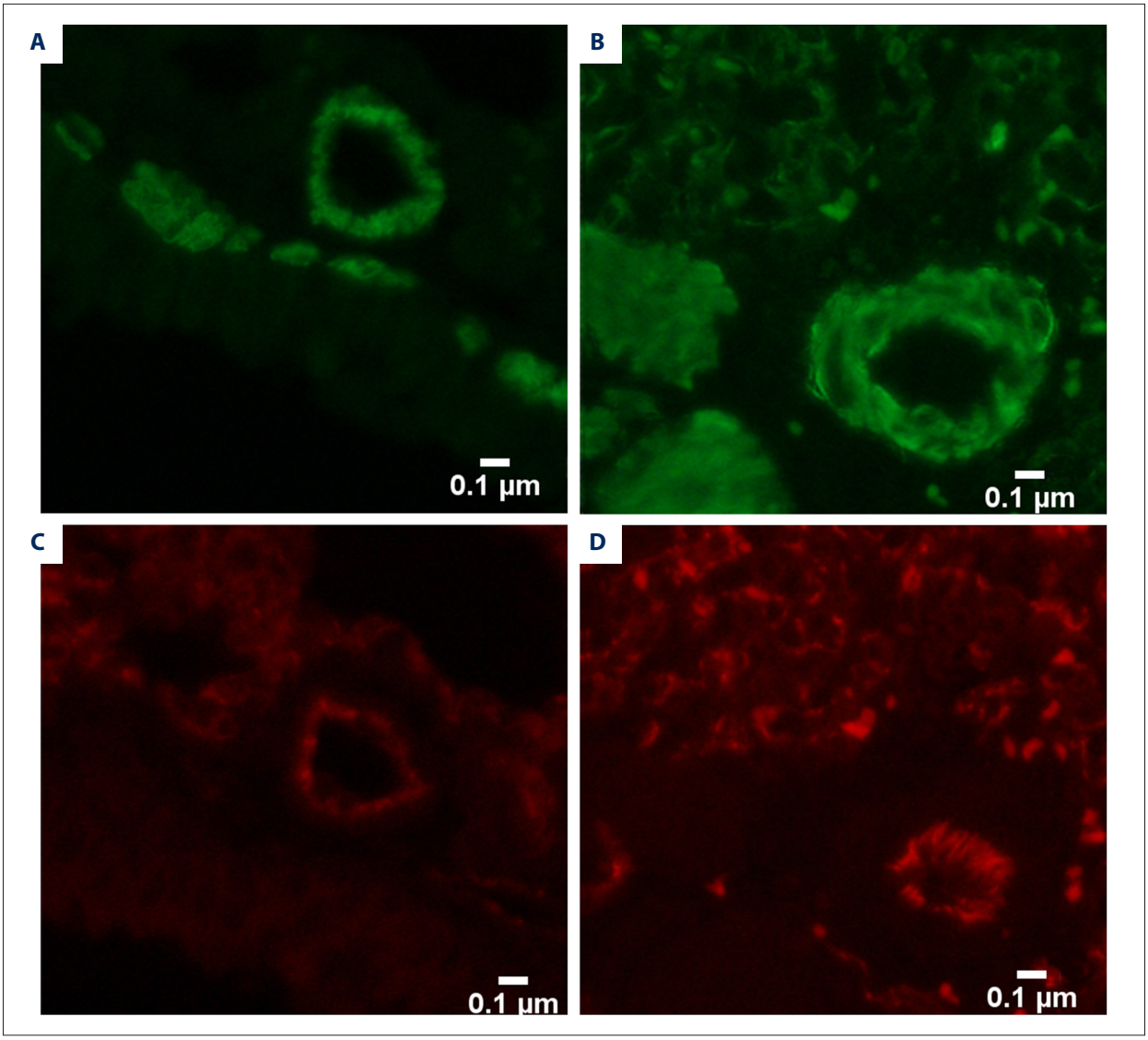

Figure 5. Pulmonary vascular remodeling in the 12th week. (**A**) Pulmonary vascular remodeling in the 12th week (×400) showing proliferation of smooth muscle cells (stained in green) in the small shunt group; (**B**) Pulmonary vascular remodeling in the 12th week (×400) showing obvious proliferation of smooth muscle cells (stained in green) in the heavy shunt group; (**C**) Pulmonary vascular remodeling in the 12th week (×400) showing a monolayer of endothelial cells (stained in red) in the small shunt group; and (**D**) Pulmonary vascular remodeling in the 12th week (×400) showing proliferation of endothelial cells (stained in red) in the heavy shunt group.

Conclusions

Our study findings suggest that abdominal aortocaval shunt in mice can lead to pathological changes in the pulmonary vessels, which are similar to those observed in human cases of shunt-associated PAH (e.g., right ventricular hypertrophy and pulmonary vascular remodeling). A direct incision of the septum of the abdominal aorta and inferior vena cava increases the shunt patency rate and leads to more advanced pulmonary vascular remodeling, providing a new platform for the in-depth study of PAH associated with CHD.

Acknowledgment

We wish to express gratitude to Prof. Xu, who gave valuable suggestions and advice, and made necessary corrections. We are greatly indebted to Dr. Zhiyu Feng, who helped overcome difficulties in establishing the animal model. Finally, we thank our colleague Lei Ding, who was responsible for taking care of the animals.

Conflicts of interest:

None.

Indexed in: [Current Contents/Clinical Medicine] [SCI Expanded] [ISI Alerting System] [ISI Journals Master List] [Index Medicus/MEDLINE] [EMBASE/Excerpta Medica] [Chemical Abstracts/CAS]

References:

1. Lowe BS, Therrien J, Ionescu-Ittu R et al: Diagnosis of pulmonary hypertension in the congenital heart disease adult population impact on outcomes. J Am Coll Cardiol, 2011; 58: 538–46
2. Diller GP, Gatzoulis MA: Pulmonary vascular disease in adults with congenital heart disease. Circulation, 2007; 115: 1039–50
3. Schulze-Neick I, Deanfield J: Pulmonary arterial hypertension in adults with congenital heart disease: General overview of disease mechanisms. Advances in Pulmonary Hypertension Autumn, 2007; 6: 121–25
4. Canniere DD, Stefanidis C, Brimioulle S, Naeije R: Effects of a chronic aortopulmonary shunt on pulmonary hemodynamics in piglets. J Appl Physiol, 1994; 77: 1591–96
5. van Albada ME, Schoemaker RG, Kemna MS et al: The role of increased pulmonary blood flow in pulmonary arterial hypertension. Eur Respir J, 2005; 26: 487–93
6. Rubin LJ: Are animal models of pulmonary hypertension relevant to the clinical disease? J Am Coll Cardiol, 2016; 67: 2047–49
7. Linardi D, Rungatscher A, Morjan M et al: Ventricular and pulmonary vascular remodeling induced by pulmonary overflow in a chronic model of pretricuspid shunt. J Thorac Cardiovasc Surg, 2014; 148: 2609–17
8. Suen CM, Zhai A, Lalu MM et al: Efficacy and safety of regenerative cell therapy for pulmonary arterial hypertension in animal models: a preclinical systematic review protocol. Syst Rev, 2016; 5: 89
9. Liu X, Meng L, Li J et al: Secretory clusterin is upregulated in rats with pulmonary arterial hypertension induced by systemic-to-pulmonary shunts and exerts important roles in pulmonary artery smooth muscle cells. Acta Physiol (Oxf), 2015; 213: 505–18
10. Ivy DD, McMurtry IF, Colvin K et al: Development of occlusive neointimal lesions in distal pulmonary arteries of endothelin b receptor-deficient rats: Anew model of severe pulmonary arterial hypertension. Circulation, 2005; 111: 2988–96
11. Taraseviciene-Stewart L, Kasahara Y, Alger L et al: Inhibition of the VEGF receptor 2 combined with chronic hypoxia causes cell death-dependent pulmonary endothelial cell proliferation and severe pulmonary hypertension. FASEB J, 2001; 15: 427–38
12. Greenway S, van Suylen RJ, Du Marchie Sarvaas G et al: S100A4/Mts1 produces murine pulmonary artery changes resembling plexogenic arteriopathy and is increased in human plexogenic arteriopathy. Am J Pathol, 2004; 164: 253–62
13. Okada K, Tanaka Y, Bernstein M et al: Pulmonary hemodynamics modify the rat artery response to injury: A neointimal model of pulmonary hypertension. Am J Pathol, 1997; 151: 1019–25
14. Dickinson MG, Bartelds B, Molema G et al: Egr-1 expression during neointimal development in flow-associated pulmonary hypertension. Am J Pathol, 2011; 179: 2199–209
15. Rungatscher A, Linardi D, Milani E et al: Chronic overcirculation-induced pulmonary arterial hypertension in aorto-caval shunt. Microvasc Res, 2014; 94: 73–79
16. Lévy M, Maurey C, Celermajer DS et al: Impaired apoptosis of pulmonary endothelial cells is associated with intimal proliferation and irreversibility of pulmonary hypertension in congenital heart disease. J Am Coll Cardiol, 2007; 49: 803–10
17. Sakao S, Tatsumi K, Voelkel NF: Reversible or irreversible remodeling in pulmonary arterial hypertension. Am J Respir Cell Mol Biol, 2010; 43: 629–34
18. Garcia R, Diebold S: Simple, rapid and effectivemethod of producing aortocaval shunts in the rat. Cardiovasc Res, 1990; 24: 430–32
19. Linardi D, Rungatscher A, Morjan M et al: Ventricular and pulmonary vascular remodeling induced by pulmonary overflow in a chronic model of pretricuspid shunt. J Thorac Cardiovasc Surg, 2014; 148(6): 2609–17
20. Xiong M, Yao JP, Wu ZK, Liao B: Fibrosis of pulmonary vascular remodeling in carotid artery-jugular vein shunt pulmonary artery hypertension model of rats. Eur J Cardiothorac Surg, 2012; 41(1): 162–66
21. Chen S, Rong M, Platteau A et al: CTGF disrupts alveolarization and induces pulmonary hypertension in neonatal mice: Implication in the pathogenesis of severe bronchopulmonary dysplasia. Am J Physiol Lung Cell Mol Physiol, 2011; 300: L330–40
22. Hopkins WE, Waggoner AD: Severe pulmonary hypertension without right ventricular failure: The unique hearts of patients with Eisenmenger syndrome. Am J Cardiol, 2002; 89: 34–38
23. Smadja DM, Gaussem P, Mauge L et al: Circulating endothelial cells: A new candidate biomarker of irreversible pulmonary hypertension secondary to congenital heart disease. Circulation, 2009; 119: 374–81
24. Huang H, Zhang P, Wang Z et al: Activation of endothelin-1 receptor signaling pathways is associated with neointima formation, neoangiogenesis and irreversible pulmonary artery hypertension in patients with congenital heart disease. Circ J, 2011; 75: 1463–71
25. Diller GP, Gatzoulis MA: Pulmonary vascular disease in adults with congenital heart disease. Circulation, 2007; 115: 1039–50
26. Thibault HB, Kurtz B, Raher MJ et al: Noninvasive assessment of murine pulmonary arterial pressure: Validation and application to models of pulmonary hypertension. Circ Cardiovasc Imaging, 2010; 3: 157–63

Indexed in: [Current Contents/Clinical Medicine] [SCI Expanded] [ISI Alerting System] [ISI Journals Master List] [Index Medicus/MEDLINE] [EMBASE/Excerpta Medica] [Chemical Abstracts/CAS]